e-Prime - Advances in Electrical Engineering, Electronics and Energy 4 (2023) 100169

Contents lists available at ScienceDirect

e-Prime - Advances in Electrical Engineering, Electronics and Energy

journal homepage: www.elsevier.com/locate/prime

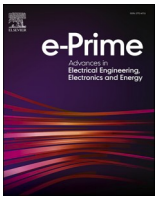

Offshore wind farm layouts designer software's

Meysam Majidi Nezhad [a,*], Mehdi Neshat [b], Maher Azaza [a], Anders Avelin [a], Giuseppe Piras [c], Davide Astiaso Garcia [d]

[a] School of Business, Society & Engineering, Department of Sustainable Energy Systems, Mälardalen University, Västerås, SE 72123, Sweden
[b] Center for Artificial Intelligence Research and Optimization, Torrens University Australia, Brisbane, Australia
[c] Department of Astronautics, Electrical and Energy Engineering (DIAEE), Sapienza University of Rome, 00184 Roma, Italy
[d] Department of Planning, Design, Technology of Architecture, Sapienza University of Rome, Via Flaminia 72 – 00196 Rome, Italy

ARTICLE INFO

Keywords:
Wind energy
Offshore wind farm layouts
Layouts designer software's
Persian gulf

ABSTRACT

Offshore wind energy can be considered one of the renewable energy sources with high force potential installed in marine areas. Consequently, the best wind farm layouts identified for constructing combined offshore renewable energy farms are crucial. To this aim, offshore wind potential analysis is essential to highlight the best offshore wind layouts for farm installation and development. Furthermore, the offshore wind farm layouts must be designed and developed based on the offshore wind accurate assessment to identify previously untapped marine regions. In this case, the wind speed distribution and correlation, wind direction, gust speed and gust direction for three sites have been analyzed, and then two offshore wind farm layout scenarios have been designed and analyzed based on two offshore wind turbine types in the Northwest Persian Gulf. In this case, offshore wind farm layouts software and tools have been reviewed as ubiquitous software tools. The results show Beacon M28 and Sea Island buoys location that the highest correlation between wind and gust speeds is between 87% and 98% in Beacon M28 and Sea Island Buoy, respectively. Considerably, the correlation between wind direction and wind speed is negligible. The Maximum likelihood algorithm, the WAsP algorithm, and the Least Squares algorithm have been used to analyze the wind energy potential in offshore buoy locations of the Northwest Persian Gulf. In addition, the wind energy generation potential has been evaluated in different case studies. For example, the Umm Al-Maradim buoy area has excellent potential for offshore wind energy generation based on the Maximum likelihood algorithm, WAsP algorithm, and Least Squares algorithm.

1. Introduction

Electricity is essential for individuals, companies, and institutions and directly linked to the country's development [1]. Nowadays, the extreme dependence on this source is indisputable since the various economic activities and social welfare performance are directly linked to electricity consumption [2]. These renewable energy sources are rapidly used nowadays, which is possible because of the conventional fossil fuels degradation, and now all energy sectors are more focused on Renewable Energy Source (RESs) penetration [3]. The current challenges associated with conventional energy sources (natural gas, oil, and coal) are climate change, fuel dependency, economy, and integration of renewable energy sources [4].

Renewable energy inclusion in the conventional grid system and the power system's various aspects of digitalization have precipitated the traditional grid system transformation to a smart grid [5]. Key to the smart grid implementation is multiple communication technologies. The communication technologies emerging dominance in power systems applications is pivotal to modernizing the conventional grid system [6]. The worldwide increase in energy demand and the high rate of limited traditional energy sources depletion has resulted in catastrophic climate change effects [7]. Fossil fuel depletion and the global warming environmental effects are the main drivers behind renewable's rapid penetration [8] in the electricity mixes worldwide [9], such as wind [10] and solar [11]. The renewables share in electricity production is projected to be 86% by 2050, up from 26% in 2018 [12].

Offshore Wind Energy (OWE) has many advantages, such as stability, availability in large quantities and predictable behavior for designing concepts and installing new technologies [13]. The first Offshore Wind Farm (OWF) was set up in Vindeby (1991), Denmark. The Vindeby OWF comprises 9450 kW turbines installed using a gravity base foundation. In addition to Vindeby OWF, another farm with similar characteristics was

* Corresponding author.
E-mail address: Meysam.majidi.nezhad@mdu.se (M. Majidi Nezhad).

https://doi.org/10.1016/j.prime.2023.100169
Received 23 January 2023; Received in revised form 9 May 2023; Accepted 12 May 2023
Available online 13 May 2023

set up in Tunø Knob in 1995 [14]. In this regard, Offshore Wind (OW) speeds on the oceans are generally higher, faster and more stable than wind speeds in coastal and terrestrial areas, and also wind shear and turbulence in offshore locations are lower due to lack of elevation [15]. In addition, these areas have more space for installation and sawing facilities of farms from coastal and land areas [16]. In this regard, wind turbines are organized in an OWF, which can include several units to two hundred OW turbines. These OWFs are usually located in scattered geographies and carefully selected based on the target sites' wind potential. One of the essential factors in the offshore site's location is to consider the distance between the fields and the prevailing wind location to maximize the electrical energy produced by the wind farm and receive more substantial and moderate winds. Therefore, designing an OWF survey requires knowledge of local and regional wind conditions.

The two main steps in the OWFs successful design play a critical role that all stakeholders will carefully implement. The first step to a successful design is to select offshore sites through national authorities. At this stage, various logic in natural sources, shipping lines, oil exploration areas, lighthouse cones, the dangers of unexploded ordnance or the chance of finding archeological remains are carefully evaluated. Then, the beach ovens are selected and announced in an open call for tenders. In the second phase, developers, and energy stakeholders to OWF design. These developers will consider OWF design, cabling, operating costs, and maintenance, depending on wind, wave, and seabed conditions, the foundations availability, and the turbine and installation vessel types to be installed. In addition, the price offered per kilowatt-hour produced (kilowatt-hours) is another critical factor.

On the other hand, the transmission system operator will provide a suitable network connection point in the OWF vicinity, awarded to the cheapest bidder for OWFs. Then, the detailed wind farm design process will continue, including in-depth seabed surveys, contracts and services of hardware suppliers, detailed farm planning, and commissioning and installation. In the last step, the operator will review and evaluate the transmission system's compliance with the network code and the supplier payment. Then, the OWF will be operational for the next 25 years and generate the most comprehensive human electricity needs [14].

The most important parameter for evaluating wind farms can be considered wind speed in offshore areas [17]. Accurate wind speed estimation is essential for all aspects of the wind energy assessment because wind energy is directly related to wind speed. Wind speed frequency analysis is essential to gain knowledge about wind energy at a particular site. Therefore, wind speed frequency analysis is essential to gain knowledge about wind energy at a particular site. The selected site wind power potential and the project econometrics can be evaluated using data distribution. Wind speed forecasting is usually done using probability distribution functions [18]. Several probability density functions such as Weibull, Rayleigh, Gamma, Beta, Gaussian [19] and Log-normal distributions can be used to indicate wind speed frequency [20]. In particular, the Weibull probability distribution is frequently applied [21] due to its simplicity and adequate representation of wind speed changes over time [22].

In short, the wind characteristics knowledge in a particular place (farm site) will lead to the efficient use of wind energy [23]. Therefore, wind speed distribution is one of the most critical aspects of wind source evaluation, which causes the OWF site operational performance continuation to depend on thorough knowledge [24]. Literary studies show that many studies have been published on the probability distribution variability used to describe wind speed frequency distribution [25]. The two-parameter Weibull function has been the most common distribution in wind energy evaluation [26]. In addition, an alternative method known as the Measurement-Correlation-Prediction (MCP) method has been developed for sampling long-term wind data at the desired farm site. MCP is typically used to link and adjust on-site measurements and long-term reference data.

The MCP method is widely used in OWF energy studies [27], especially to evaluate the wind potential of sites that do not have long-term local wind data. Wind source assessments are usually based on historical climate observations, numerical simulations, satellite-based remote sensing, and reanalysis data. Historical observations of wind energy refer to using tools to measure wind speed and direction to determine a particular location, which is limited by the point observation range evaluation type [28]. On the other hand, in addition to relative flexibility, simplicity, and accuracy, numerous comparative analyzes suggest [29] that the Weibull distribution may not always be suitable for all wind regimes [30]. Several studies claim that mixed distributions show a significant advantage in the wind regime results over conventional non-mixed distributions [31]. Otherwise, with increasing parameters and model complexity, using different mixtures is not easy and even, in some cases, is not applicable [32]. On the other hand, several attempts should be made to select the correct parameter estimation method because of the analysis's accuracy, feasibility and reliability [33].

According to state of the art described above, firstly, a review of layout design software and tools for offshore wind farms has been done with an approach focused on existing scientific gaps. Secondly, using the data collected from existing buoys, two scenarios for the layout design of an offshore wind farm have been evaluated based on the two offshore wind turbines' selected characteristics in the Northwest Persian Gulf. Considering the new aspects of the research, it is essential to emphasize that there are no case studies on offshore farm design using data that have been fully validated. In this case, it can be mentioned that despite having good potential in the Persian Gulf, unfortunately, this region lacks measuring buoys in marine areas [34]. On the other hand, many of the used buoys have insufficient data quality due to the delay in calibration. This factor can be considered the main factor behind the unknown offshore wind potential in the Persian Gulf [35]. Furthermore, long-term recorded data is unavailable in most marine areas according to the abovementioned factors. Therefore, this study can be considered the first study on the offshore wind farms layout design in the Northwest Persian Gulf. In this regard, the data is reliable and has been evaluated for decision-making, and the power distribution probability distribution, energy density, and power capacity factors of two commercial wind turbines were presented to support the installation's decision-making process. The rest of this paper is structured as follows. In Section 2, the wind farm designer software innovation is introduced. The case study is presented in Section 3, and the material and methods are presented in Section 4. Results and discussions are described in Section 5, respectively. In Section 6, the offshore wind turbine structure lessons are proposed. Finally, concluding remarks are presented in Section 7.

2. Wind farm designer software innovation

Researchers today use micro-scale numerical simulation software to study and simulate wind sources to overcome the surface-based wind monitoring systems costs and inconveniences. In this regard, WAsP, MM5, MesoMap, Site Wind, TAPM and WEST are simulation tools that are widely used. In addition, many researchers mainly use integrated model systems to evaluate wind energy sources. Such systems use a medium-scale numerical meteorological model, the Climate Research and Forecasting Model (WRF) or MM5, the Complex Earth Dynamics Detection Model, the California Meteorological Model, or the Advanced Regional Forecasting System [36]. However, the most popular and widely used software products are Computational Fluid Dynamics (CFD)-based software for OWF design, such as Meteodyn WT and WindSim. Scientific studies and practical engineering experiments show that CFD-based computing software can simulate wind sources more accurately than WAsP [37].

The popularity of using open software can be attributed to the Weibull distribution used to provide output results [38]. For example, a study of medium-scale wind data used Meteodyn WT software to assess wind conditions on Phaluay Island in Thailand with a spatial resolution of 90 m. This study shows that the software results are precisely consistent with wind data on a medium scale [39]. Another study using

Meteodyn WT to evaluate a wind farm in complex terrain found that the Meteodyn WT wind source assessment was almost entirely consistent with locally measured data, but the wind speed simulation was conservative [40]. WindSim simulation software can correctly solve and develop nonlinear energy equations. Therefore, WindSim software allows places with complex lands and local weather conditions to be simulated. For example, researchers constructed more than 120 land models from data on the Norwegian coast altitude and ruggedness from southern Lindens to the northern border with Russia and used them to assess wind sources off the Norway coast [41].

In this case, WindMap/OpenWind software has been used in many wind atlases' first descriptions in various regions [42]. However, published articles on using these comparative tools with WindSim are minimal. Perhaps the main factor limiting the tool use can be found in the cost of purchasing a license for the software. Castellani et al. [29] simulated flow at two wind farm sites using WindSim CFD and a mass storage model and based their findings on a data set in southern Italy. They compared the monitoring control and data collection of turbines (SCADA). Proietti et al. [43] also used WindSim software in their study to estimate the wind potential in combined wind and solar operation projects in remote areas. Dutra and Szklo [44], and Pérez et al. [45], compared the software outputs with data from a wind farm located on low-lying land in Switzerland, considering that both models confirmed the k-ε and k-ω turbulence.

Different OWF design tools use analytical awakening models [46] or CFD flow solvents. In this case, analytical wake-up models have been developed and implemented to predict power losses in operational farms [47]. In addition, analytical wake models are simplified and require much less computational time to estimate wind farm sources and power losses to wake up than in the past. These models include algebraic equations for turbine-induced peak velocities and multiple turbine overlaps. Some analytical wake models, such as the Park model [48], are implemented in industry-standard software, such as the Wind Atlas Analysis and Application Program (WAsP), WindPro, and WindFarmer to evaluate wind sources and wind turbine's micro-location.

In this regard, another method for CFD solvents based on intermediate solutions or NaviereStoke equations has been developed and improved, such as EllipSys3D [49], Fuga [50], and WIRE-LES [51]. The wind turbine influential forces in these equations are finally parameterized and simulated using the 1D momentum theory or the blade element. Barthelemy et al. [47] used CFD-based analytical models to predict wind turbine power losses in different wind directions. However, the predicted output power results were less than 10° error with the observed data for wind. Specifically, the projected power outputs are considered up to 55% at a complete standstill, where the wind direction is parallel to the turbine rows. These differences indicate the need to improve the wind farm design tools and wind turbine parameterization turbulence modeling.

In recent years, modern CFD tools have been essential for modeling wind flow on complex terrains (with high elevations) [52]. Therefore, these models can provide information about specific locations, altitudes, time and wind power estimates. Most uses for flatland or gentle hills have a decent output to indicate that it works correctly, but problems can arise when it comes to complex mountaineering (steep and steep hills). Recently [53], WindSim and OpenFOAM CFD software have analyzed wind currents in some complex hilly terrains. However, after performing several comparative experiments and flow scenarios using both software, the researchers concluded that WindSim is more suitable for analyzing wind flow on uneven terrain with multiple roughness factors. Wind conditions with standard linear models such as WASP do not sufficiently reproduce wind conditions in complex fields [54]. Furthermore, even on-site anemometer measurements do not necessarily provide the results required for production calculations because wind speed extensions at wind turbine hub heights are incorrect [55]. Table 1 reviewed the studies regarding the subject approaches main categories, the methods and the tools used. This makes it possible to identify existing trends and potential new fields of study while also considering how to compile modeling lessons and perform future review exercises.

Table 1
Overview of the articles surveyed corresponding classification and methods.

Topic	Modeling tool	Method	Ref
Wind atlas	WindMap / OpenWind	Terrain elevation and local surface roughness	[42]
Wind Flow	WindSim (CFD) and mass consistent	RANS/GCV	[56]
Wind and solar	CFD/GeoNetwork	General Collocated Velocity	[43]
Wind field and farm power	WindSim (CFD)	Turbulence/forest/ wake models	[57]
Operation optimizing	GIS model	Rule-based	[44]
Turbulence	A simple linear	Measure-Correlate-Predict	[45]
Power Loss	WAsP, CRES, WindFarmer, WAKEFARM, CENER, NTUA	Analytical	[47]
Wind Flow	WindSim/OpenFOAM	RANS	[53]

3. Case study

The Persian Gulf has the warmest water [58] in the world [59]. Studies in sea level temperature used to measure global warming related to climate change show this well [60]. The Persian Gulf is a long, flat, shallow semi-enclosed basin between 24 and 30° north and 48 to 57° east. The basin varies in width from 56 to 338 km, while the length of its central axis is about 990 km. Its total area is about 226,000 km^2s, and the average water depth is about 35 m [61]. In the Persian Gulf, the meteorological environment main component in the northwest, solid northwest winds from the cold fronts pass through eastern Turkey and the mountains of northern Iraq and pass through the Kuwaiti desert to this region. This seasonal wind event occurs mainly in summer and winter [62]. Northerly winds may last for several weeks, but they can sometimes be accompanied and interrupted by southeast winds called high-humidity couscous. The World Meteorological Organization (WMO) Committee has stated that the temperature recorded at 54.0 °C at a ground station in Mitriba-Kuwait recorded the highest temperature [63].

Kuwait has a coastline of about 496 km [64]. Kuwait often has a desert climate with significant differences in daily and seasonal temperatures [65]. The total area of Kuwait's territorial waters is about 9700 km^2s [66]. The Kuwait offshore environmental conditions are generally suitable for commercial facilities because the seawater depth is shallow, and there is no storm trace. The maximum water depth in Kuwaiti territorial waters is only about 30 m. The importance given to offshore wind energy commercialization is our primary motivation for assessing the wind power potential in Kuwaiti territorial waters and identifying suitable locations for installing wind turbines. In this regard, although the Persian Gulf has good potential for offshore wind energy areas, this energy source has not yet been considered for reasons such as the quality data lack in these areas. The main reason is the historical data and the lack of accurate on-site instrument observations in marine areas. On the other hand, the investment growth in offshore wind energy has motivated various efforts to evaluate offshore wind sources to find and target investment opportunities. As a result, some OW source assessments have been performed using various reanalysis data, locally measured data, meteorological models, or a dataset combination [67]. Three in-situ OW buoys data have been analyzed, including wind speed and wind direction with 10 min resolutions from a year of the Persian Gulf. Three studied buoys (Fig. 1) can be considered spatially in offshore marine areas, and Table 2 shows the three studied buoys' characteristics.

In the second phase, two turbines were selected according to the

Fig. 1. The Northwest Persian Gulf offshore buoys locations. (For interpretation of the references to color in this figure legend, the reader is referred to the web version of this article.)

Table 2
Three studied buoys' characteristics measurement.

Station name	Latitude (N°)	Longitude (E°)	Sea Level (m)	Distance (km)	Time resolution	Data year
Beacon M28	29.51	48.60	5.93	22.88	10 Min	2012
Sea Island Buoy	29.06	48.19	4.75	16.27	10 Min	2015
Umm Al-Maradim	28.68	48.65	17.4	25.66	10 Min	2012

desired characteristics for installation in the Northwest Persian Gulf. As a result, these two turbines (Table 3) can be considered on the top list of turbines installed in offshore areas with high success.

4. Material and methods

Firstly, one-year wind speed data was used to evaluate and identify the wind-speed potential in three locations using the wind power density by applying Eq. (1).

$$P = \frac{1}{2}\rho v^3 \left(W / m^2\right) \tag{1}$$

where ρ is the standard air density at sea level, with a mean temperature of 15 °C and a pressure of 1 atmosphere (1.225 kg/ m^3), and v is the wind speed (m/s).

Secondly, Pearson's linear Correlation Coefficient (CC) [68] test was used to analyze the level of correlation between the three buoys location. The CC of the population $p_{X,Y}$ between two sets generated randomly, X and Y, are defined as follows:

Table 3
The two turbines' specifications studied for OWFs installation.

Turbine models	Characteristics
Gamesa G128–5.0 MW Offshore	Rated power: 5.000 kW Cut-in wind speed: 2.0 m/s Rated wind speed: 14.0 m/s Cut-out wind speed: 27.0 m/s Diameter: 128.0 m Number of blades: 3
REpower 5 MW Offshore	Rated power: 5.075 kW Tower height: 90 m Rotor diameter: 126 m number of blades: 3 Cut-off speed: 25/30 m/s Hub heights: 90–100 m

$$p_{X,Y} = corr(X,Y) = cov(X,Y)/\sigma_X\sigma_Y = E[(X-\mu_X)(Y-\mu_Y)]/\sigma_X\sigma_Y \quad (2)$$

where μ_X and μ_Y are the expected values of X and Y, and both σ_X and σ_Y are the standard deviations (SD). Next, the wind-speed data statistical analysis, an autocorrelation test was used [69]. The auto-CC lag k (r_k) for a sequential time series $S_1, S_2, \ldots, S_K$ was defined as follows:

$$r_k = \frac{1}{T}\sum_{t=1}^{T-k}(S_t-\overline{S})(S_{t+k}-\overline{S}) \Big/ c_0,\ k = 0,1,\ldots,L \quad (3)$$

where c_0 denotes the sample variance of the sequential data, T is the effective sample size of S_t and $\overline{S}$ is the average of data S_t. Generally, $L = T/4$, depending on the data length. As a case study, two offshore wind farm layout scenarios have been designed and analyzed based on two offshore wind turbine types' of the Northwest Persian Gulf.

5. Results and discussions

This section provides the offshore data location collection duration and related details to OW data measurement of farm layout design. In addition, the data collection elevation at each location and the offshore wind speed distribution vertical extrapolation details are provided.

5.1. Site characteristics

The wind rose plots (See Fig. 2) are proposed to investigate and extract the case studies significant wind direction characteristics. We can see that the three offshore sites' wind patterns are approximately the same, and the most considerable wind direction blew.

Fig. 3 shows the distribution (histogram) and correlation between four features, wind speed, wind direction, gust speed and gust direction for two sites, Beacon M28 and Sea Island Buoy. As expected, the highest correlation between wind and gust speeds is between 87% and 98% in Beacon M28 and Sea Island Buoy, respectively. Considerably, the correlation between wind direction and wind speed is negligible.

5.2. Offshore wind site potential output

Tables 4, 5, and 6 presents the k and A (m/s), Mean (A), Proportion Above 4.25 (m/s), power density (W/m^2) and R-Squared, Elapsed Time (ms) using maximum likelihood, least squares, WAsP, openwind algorithms.

5.3. Offshore wind turbines selection layout

Table 7 shows the mean power output, annual energy output and capacity factor value for the two turbines (Gamesa G128–5.0 MW Offshore and REpower 5 MW Offshore) before and after losses studied in the three sites. This comparison shows that both turbines can be appropriately installed in the offshore marine areas, but in this prioritization, the sea island zone produces more energy for both turbines due to the wind speed.

5.4. Offshore wind farm layout map and energy output

An irregular arrangement achieves the turbine's placement. This allowed for minimizing the wake effects between the turbines in areas close to the size. So, in the irregular layouts, the results depend on how the turbines are arranged. In contrast, the most expansive arrangements give the regular layout best results. These values are higher than the configuration power output calculated for the most extensive configuration. Therefore, the increase in the OWF generates a size less profitable gain when the power output increases moderately. Fig. 4 shows the proposed wind farm concerning the prevailing wind direction. In addition, Table 8 compares the two types of wind turbine output.

6. Offshore wind turbine structure lessons

One of the most critical challenges in developing offshore wind farms is selecting the farm's structure type [70]. The following sections provide an overview and description [71] on fixed and floating wind turbine structure types offshore wind turbine lessons [72];

6.1. Fixed wind turbine structures

in the offshore wind energy industry have successfully developed in the oil and gas industry using successful experiences and technologies. Each of the foundations, explanations of the constituent structure and installation methods and other installation considerations in the seabed water depth and geology have been examined. All types of wind turbine foundations should have the following two characteristics, a) vertical loads from the weight of wind turbine components: offshore wind turbine foundations must withstand vertical loads so that the wind turbine does not sink into the sea, b) horizontal loads from wind force ocean currents and waves: the wind turbines foundation must withstand horizontal loads to prevent slipping on the seabed. In addition, when choosing the foundation type, the wind turbines number in the desired area should be considered.

a) *Monopile Foundations,* many OWFs around the world have been commissioned using integrated foundations. The structure consists of a large-diameter steel pipe and a base for vertical and lateral support into the seabed in the offshore areas. The Monopile Foundations structure, the soil resistance at the monopile and the base sides friction with the surrounding soil are used to carry vertical loads. The structure depends on the factors size such as water depth, soil resistance at the seabed, the turbine size, the wind turbine weight, the area occupied by the wind turbine blades, and the wave and weather conditions area. The structure is designed to include steel pieces with a diameter of about 10 m (33 feet) and is currently recommended for use in water up to 50 m (164 feet). Natural currents in the oceans and seas can cause the bed soil to move around the monopile, which can cause depressions or voids around the wind turbine's foundation. This is because the structural strength in the seabed depends on the surrounding soil strength. Therefore, builders usually design a rock bed around the foundation used to prevent the loss of soil around it. Usually, the rock layer diameter is about 50 m (164 feet), and the thickness is 1–1.5 m (3–5 feet) [73,74].
b) *Jacket Foundations,* the Jacket foundations used in offshore wind turbines have a lattice truss structure like the system designed for offshore oil extraction platforms. The Jacket foundations structure typically has four pillars. The tubular bases at the corners are made of smaller diameter cross-sections using diagonal joints welded between the legs to increase their strength. The diameter of the tubular steel members that make up the bases is often 1 to 3 m (3.3 to 10 feet), much smaller than the integrated diameters. Above the waterline, a steel transmission piece distributes the turbine tower

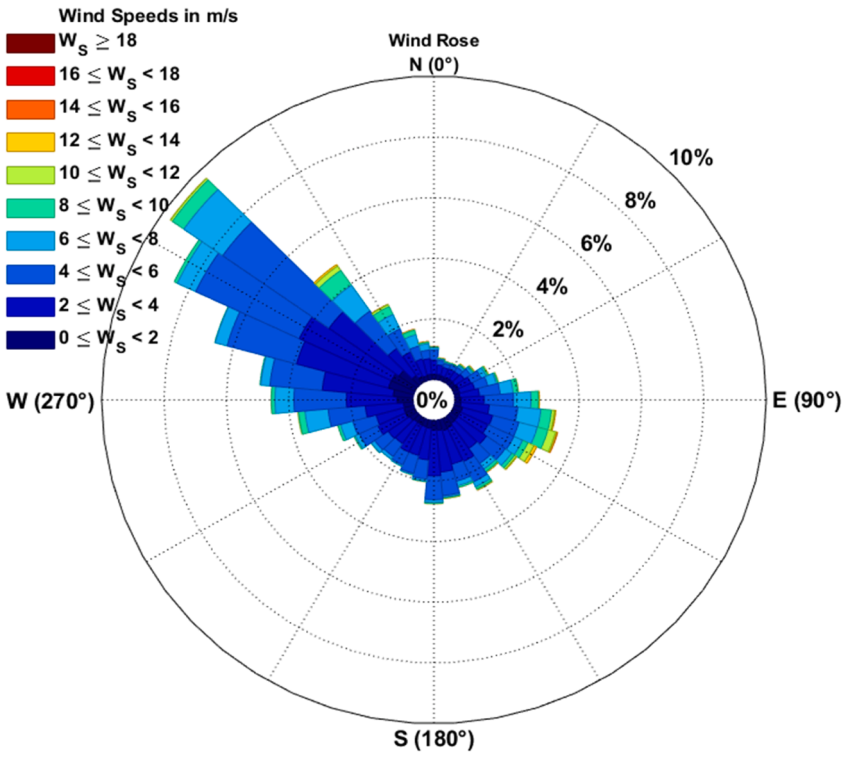

(a)

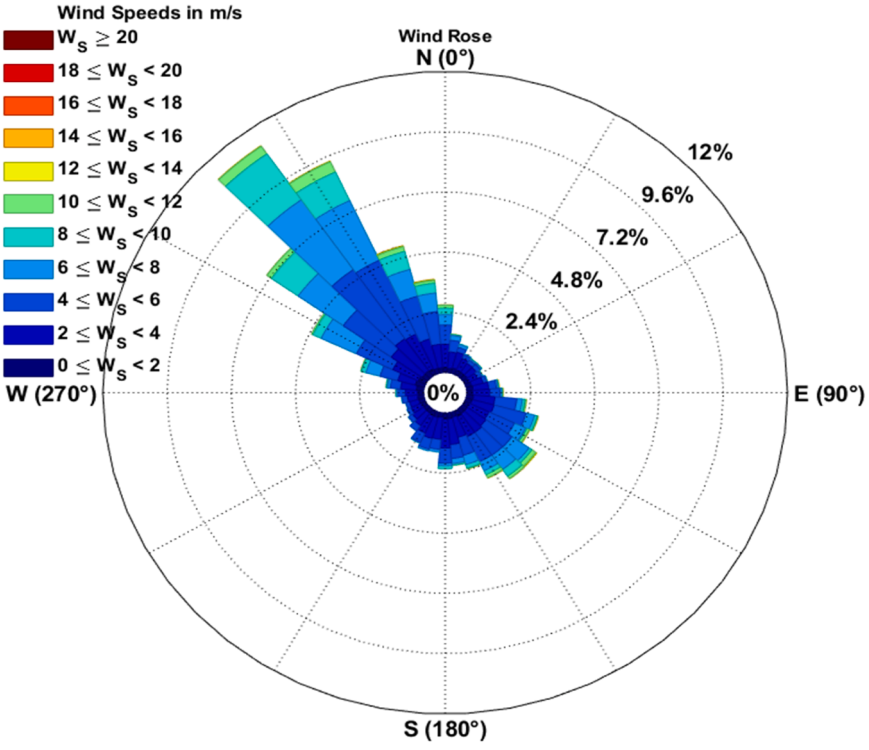

(b)

Fig. 2. Wind speed and wind direction distribution, (a) Beacon M28, (b) Sea Island Buoy, and (c) Umm Al-Maradim sites. (For interpretation of the references to color in this figure legend, the reader is referred to the web version of this article.)

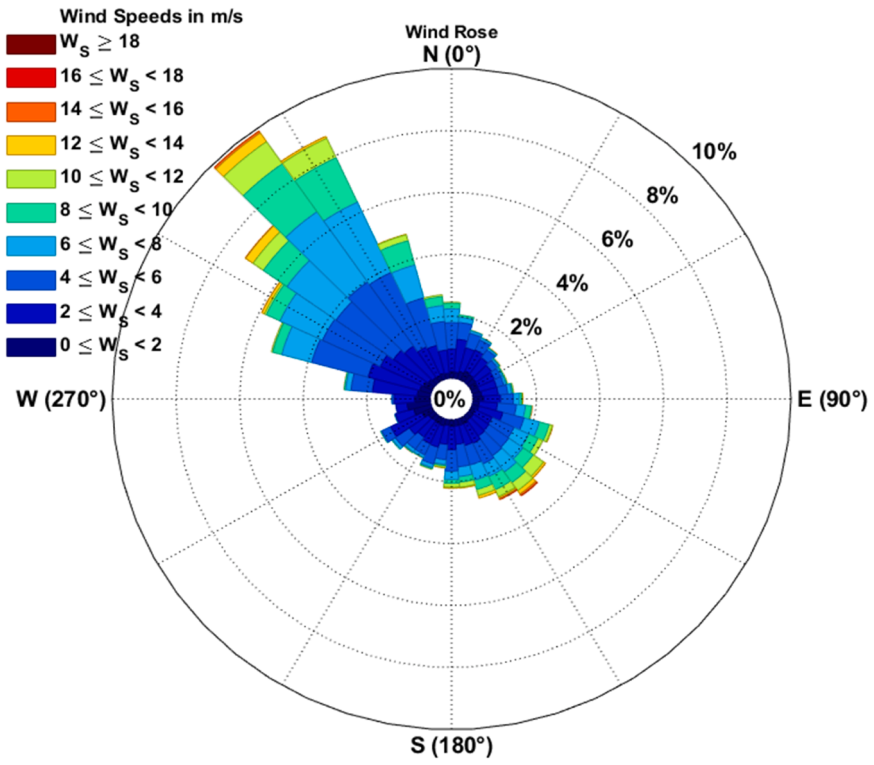

(c)

Fig. 2. (*continued*).

weight to the Jacket foundations. Jacket foundations typically carry vertical loads to the seabed using pipe bases. The combined bases neutralize the horizontal forces created to overturn this structure [73].

c) *Tripod Foundations,* a tripod foundation has many characteristics of a jacket foundation and some of the Monopile foundations characteristics. A tripod foundation has a pyramidal structure made of tubular steel parts. Like the jacket base, the bases anchor in the tripod foundation corners in a triangular shape on the seabed. The legs are typically 20 m (66 feet) to 40 m (131 feet) apart. A diagonal brace connects each base to a central cylindrical column that resembles a single piece. The difference structure is that the central pillar does not enter the sea. Instead, the tripod supports the central column structural members in an interconnected manner and holds it above the water line to provide a base for the turbine tower. The tripod transmits vertical loads to the seabed through the pedestals. Like the jacket structure, this structure has good resistance to creating horizontal forces that can cause overturning [73].

d) *Tri-pile Foundations,* a tri-pile foundation structure, consists of a cylindrical tripod with a converter connected at the waterline top. The tri-pile foundation structure forms a space frame that supports the wind turbine structure well. The convertible piece connects the three base retaining masses below the water line to hold the wind turbine tower structure above the water level. The tri-pile foundation structure legs are very similar to the monopiles structure. The difference is that the bases diameter is smaller. They are usually about 3 m (10 feet) in diameter. The tri-pile foundation structure location depends on several factors: water depth, wind and hydrodynamic loads, geological conditions, pipe diameter, and the foundation embedding depth. The tri-pile foundation can be used in deepwater at 25 to 40 m (80 to 130 feet) [71].

e) *Jack-Up Foundations* [75], the jack-up foundation structure is like drilling rigs used in the offshore oil and gas industry for decades and is now recommended for OWFs projects. The jack-up structure consists of a floating platform with three or four legs that can be raised and lowered relative to the central platform. The structure bases on the legs help to distribute the load from the legs to the seabed. After adjusting the bases, the ballast water is drained, and the body is connected from the water level to its operating height. Jack-up structure foundations are recommended for offshore wind turbines up to 100 m (330 feet) deep [76].

f) *Suction Bucket Foundations* [77], also known as single-level bases or monopods. Indeed, bucket foundations have a substantial diameter. Unlike the silent base of the suction bucket foundations, in which several suction hoppers may be used instead of the bases, a single base of the suction bucket is used as a single and integrated base for the entire base structure foundations platform. In their simplest form, these foundations have a cylindrical shape with an open end, a closed head and a sufficient diameter to withstand overturning the structure [71].

6.2. Floating wind turbine structure types

the floating wind turbines wind affects, so creating an aerodynamic thrust tends to tilt the platforms slightly. Therefore, all wind turbine platforms must be capable of neutralizing the instantaneous aerodynamic momentum effect. In the spar structures design, a low-level steel or concrete cylinder has been used, to easily hold the floating wind turbines gravity center below the float center. In general, spars can be called stable instruments that have good stability in stable stability due to their semi-floating capability [78]. On the other hand, the Tension Leg Platform (TLP) platform structures are highly buoyant structures developed using a traction bracing system. In these structures, bases, usually cables, have been used to provide more traction capability if there is a greater desire. This structure has effectively neutralized aerodynamic drift in a floating wind structure [79]. Here are five

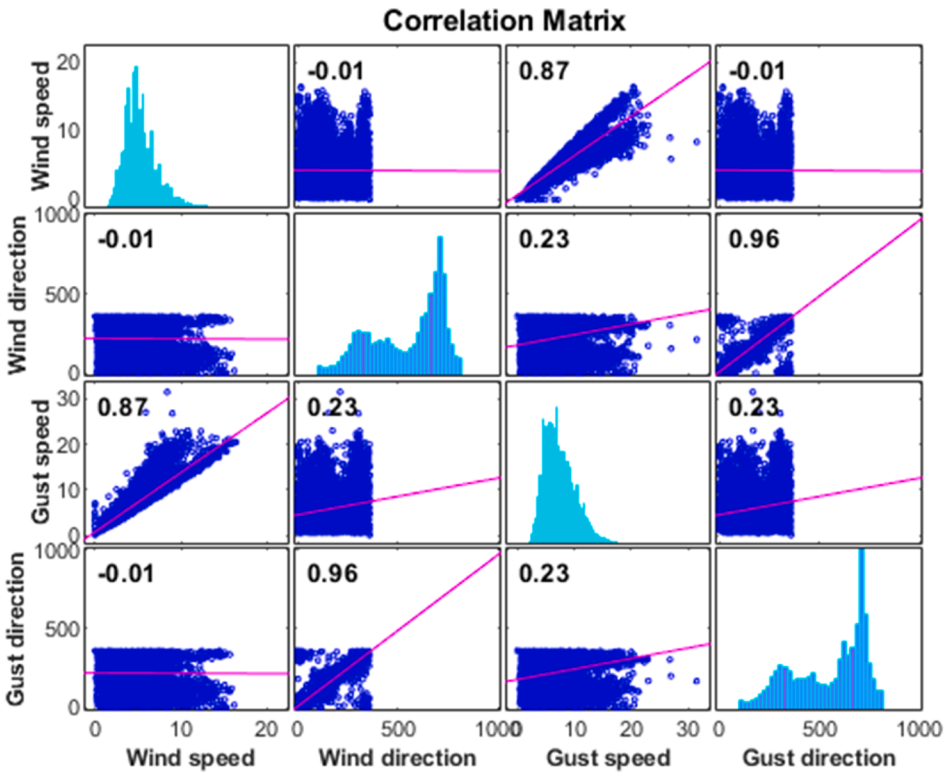

(a)

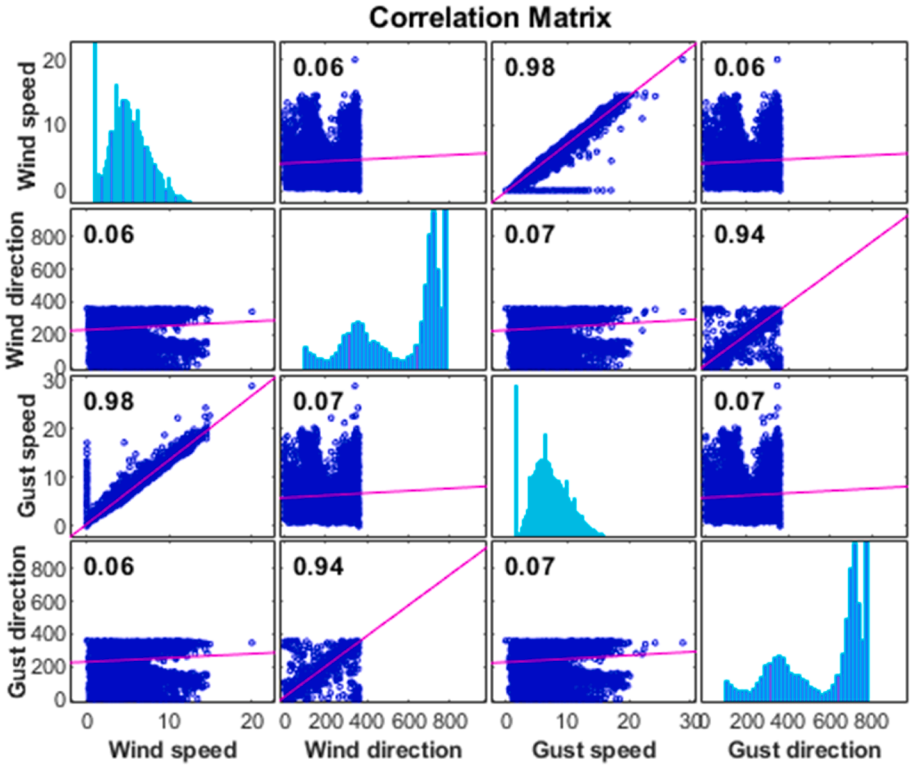

(b)

Fig. 3. Pearson's CC between pairs of wind speed, wind direction, gust speed and gust direction, (a) Beacon M28, and (b) Sea Island Buoy sites. (For interpretation of the references to color in this figure legend, the reader is referred to the web version of this article.)

Table 4
The Beacon M 28 buoy wind speed analysis based on algorithms.

Algorithm	K	A (m/s)	Mean (A)	Proportion above 4.25 (m/s)	Power density (W/m^2)	R squared	Elapsed time (ms)
Maximum likelihood	2.111	4.804	4.254	0.462	85.5	0.9669	39
Least squares	2.274	4.783	4.327	0.466	79.1	0.9756	1
WAsP	1.897	4.671	4.145	0.433	88.0	0.9420	1
Openwind	2.042	4.798	4.250	0.458	88.0	0.9606	1
Actual data	51.540	51.540	4.250	0.433	88.0	–	–

Table 5
The Sea Island buoy wind speed analysis based on algorithms.

Algorithm	K	A (m/s)	Mean (A)	Proportion above 4.25 (m/s)	Power density (W/m^2)	R squared	Elapsed time (ms)
Maximum likelihood	1.842	4.953	4.400	0.450	108.7	0.8692	22
Least squares	1.987	4.896	4.339	0.448	96.2	0.8612	1
WAsP	1.691	4.804	4.286	0.424	111.3	0.8656	0
Openwind	1.789	4.930	4.385	0.444	111.3	0.8703	0
Actual data	39.029	39.029	4.385	0.424	111.3	–	–

Table 6
The Umm Al-Maradim buoy wind speed analysis based on algorithms.

Algorithm	K	A (m/s)	Mean (A)	Proportion above 4.25 (m/s)	Power density (W/m^2)	R squared	Elapsed time (ms)
Maximum likelihood	1.878	5.689	5.046	0.447	160.5	0.9854	32
Least squares	1.908	5.732	5.086	0.454	161.6	0.9858	2
WAsP	1.846	5.625	4.997	0.439	158.8	0.9835	1
Openwind	1.917	5.710	5.065	0.452	158.8	0.9864	3
Actual data	51.529	51.529	5.065	0.439	158.8	–	–

Table 7
OWFs energy output with two offshore turbine models of three different locations.

		Gamesa G128–5.0 MW Offshore		REpower 5 MW offshore	
Stations	Variables	Before losses	After losses	Before losses	After losses
Beacon M 28	Mean Power Output	1.295 Kw	1.100 kW	1.299 kW	1.104 kW
	Annual Energy Output	11.340.875 kWh/yr	9.639.744 kWh/yr	11.379.016 kWh/yr	9.672.164 kWh/yr
	Capacity Factor	25.9%	22%	25.6%	21.8%
Sea island	Mean Power Output	1.514 Kw	1.287 Kw	1.527 Kw	1.298 Kw
	Annual Energy Output	13.258.817 kWh/yr	11.269.995 kWh/yr	13.376.804 kWh/yr	11.370.284 kWh/yr
	Capacity Factor	30.3%	25.7%	30.1%	25.6%
Umm Al-Maradim	Mean Power Output	1.410 Kw	1.198 Kw	1.395 Kw	1.186 Kw
	Annual Energy Output	12.394.312 kWh/yr	10.496.915 kWh/yr	12.221.237 kWh/yr	10.388.052 kWh/yr
	Capacity Factor	28.2%	24%	27.5%	23.4%

concepts of the platform that are technically experimental and theoretically going through different stages of maturity:

a) *Sea Flowers* [80], are floating offshore wind platforms designed and completed by Fincantieri. Sea Flower operates a water-immersed hexagonal platform that acts as the blue float main body, using six semi-submerged blue columns at its corners. In general, lightweight concrete has been used to build the structure. Sea Flowers are very efficient using a six-lane mooring system for seabeds with a water depth of 50–200 m [81].
b) *The WindFloat platform* [82], was built and developed by Principal Power as part of the WindFloat Atlantic project [83,84]. WindFloat platform substructure is a semi-submerged structure consisting of three cylindrical columns, each at an angle of a triangle. These three cylindrical columns are restrained and connected by horizontal beams to form a truss structure. The floating wind turbine tower is mounted on one of three pillars. For this reason, the wind turbine tower base diameter should be close to the structural column diameter to reduce the leading stresses most effectively [83].
c) *The Hywind platform's* [85], structure was created and designed by Equinor (Statoil) for the HyWind Scotland project. The Hywind platform's structure is the basic building block of the spar-buoy concept and consists of a cylindrical column floating in the water. The material cylindrical column is empty of steel. This structure ensures the platform's stability against waves and strong winds. The steel structure weight often reaches 2300 tons, which, if we add the platform upper structure weight to it, its weight will reach about 10, 000 tons. The Hywind platforms structure is fixed to the seabed by anchor chains [86].
d) The Hexafloat platform [87], the floating platform is made of a hexagonal structure using steel cylinders, with a central column on the wind turbine structure. The equilibrium weight in this structure is made of cylindrical steel (iron powder with a density of 5200 kg/m^3). The Hexafloat platform usually uses three to six chains or anchors fixed to the floor at sea. The main advantage of this structure is its flexibility to install different wind turbines (2 to 15 MW) on itself. In addition, this structure is new to other structures and can mass-produce due to lower costs and less energy.

7. Conclusions

One of the renewable energy sources is the using wind energy potential, which has reached maturity and high competitiveness in different land and sea areas, mainly with the new technology's

Turbine per row	10
Number of rows	2
Turbine spacing	8 Rotor diameters
Row spacing	8 Rotor diameters
Offset for rows	4 Rotor diameters
Row orientation	48 degrees

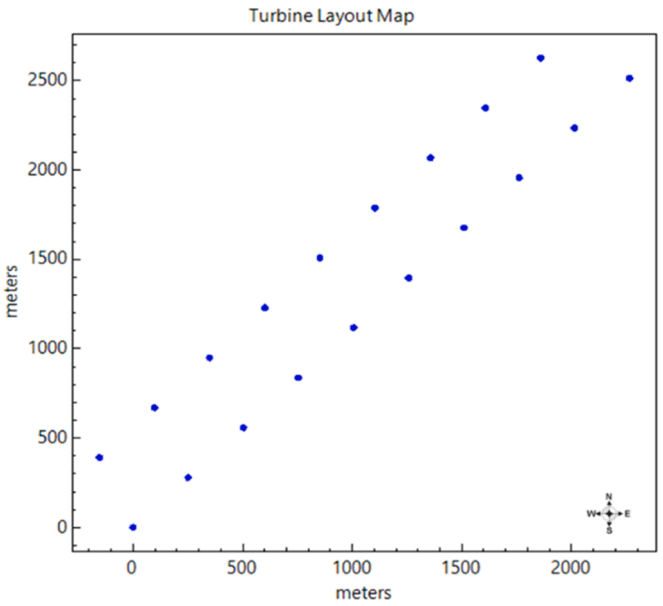

Fig. 4. The Persian Northwest OWF layout design. (For interpretation of the references to color in this figure legend, the reader is referred to the web version of this article.)

Table 8
Two OWFs energy output of three different locations.

		Gamesa G128–5.0 MW Offshore farm		REpower 5 MW offshore farm	
Stations	Variables	Before losses	After losses	Before losses	After losses
Beacon M 28	Mean power output	25.900 Kw	22.000 kW	25.980 kW	22.080 kW
	Annual energy output	226.817.500 kWh/yr	192.794.880 kWh/yr	227.580.320 kWh/yr	193.443.280 kWh/yr
Sea island	Mean power output	30.280 Kw	25.740 Kw	30.540 Kw	25.960 Kw
	Annual energy output	265.176.340 kWh/yr	225.399.900 kWh/yr	267.536.080 kWh/yr	227.405.700 kWh/yr
Umm Al-Maradim	Mean power output	28.200 Kw	23.960 Kw	27.900 Kw	23.720 Kw
	Annual energy output	247.886.240 kWh/yr	209.938.745 kWh/yr	244.424.740 kWh/yr	206.761.040 kWh/yr

development. However, many offshore areas with good potential for wind farm installation and operation expansion remain unexplored. This article examines the wind analysis software use that can be used to analyze wind power and design wind farms. In this study, the three buoys' wind data have been used of the northwest Persian Gulf. However, it should be noted that obtaining updated and accurate data in this area is challenging due to the calibrated buoys lack. The wind speed distribution and correlation, wind direction, gust speed and gust direction for two sites, Beacon M28 and Sea Island Buoy shows that, the highest correlation between wind and gust speeds is between 87% and 98% in Beacon M28 and Sea Island Buoy, respectively. Considerably, the correlation between wind direction and wind speed is negligible. Three Maximum likelihood algorithm, the WAsP algorithm, and the Least Squares algorithm has been used to analyze the wind energy potential in offshore in-situ buoys locations of the Northwest Persian Gulf. In addition, the wind energy generation potential has been evaluated in different case studies. For example, the Umm Al-Maradim buoy area has excellent potential for OW energy generation based on three Weibull fitting algorithms (Maximum likelihood algorithm, WAsP algorithm, and Least Squares algorithm). In this article, an attempt has been made to understand the wind farm layouts' complexity better. We have investigated wind turbines' regular and irregular layouts in a large offshore wind farm and the optimization solution to select the best layout.

The offshore farm layouts designer software has been used as a "Fast and no-cost" method to identify offshore wind speed in large marine areas. This designer software can be developed by adding other essential parameters of offshore wind farm installation, such as water depth. The "Fast and no-cost" method evolution can be such that it leads to an accurate analysis of the distance between offshore wind farms at their potential cost. modeling efforts to design wind farms in the project face difficulties initial design phase in estimating the best turbine location. Some observed differences between models and reality can be attributed to the complex farm design.

Declaration of Competing Interest

The authors declare that they have no known competing financial interests or personal relationships that could have appeared to influence the work reported in this paper.

Data availability

Data will be made available on request.

Acknowledgement

The authors thank Dr S. Neelamani and Dr Y. Al-Osairi from Environment and Life Sciences Research Center, The Kuwait Institute for Scientific Research (KISR), for providing the buoy data. This research was funded by the European Union's Horizon 2020 European Green Deal Research and Innovation Program (H2020-LC-GD2020-4), grant number No. 101037643-ILIAD (Integrated Digital Framework for Comprehensive Maritime Data and Information Services). However, the article reflects only the author's view and that the Commission is not

responsible for any use that may be made of the information it contains.

References

[1] Z. Guzović, N. Duić, A. Piacentino, N. Markovska, B.V. Mathiesen, H. Lund, Paving the way for the Paris agreement: contributions of SDEWES science, Energy 263 (September 2022), https://doi.org/10.1016/j.energy.2022.125617.

[2] D.G. da Silva, M.T.B. Geller, M.S. dos Santos Moura, A.A. de Moura Meneses, Performance evaluation of LSTM neural networks for consumption prediction, e-Prime - Adv. Electr. Eng. Electron. Energy (2022), 100030, https://doi.org/10.1016/j.prime.2022.100030.

[3] S. Behera, N.B.D. Choudhury, Adaptive optimal energy management in multi-distributed energy resources by using improved slime mould algorithm with considering demand side management, e-Prime - Adv. Electr. Eng. Electron. Energy (2023), 100108, https://doi.org/10.1016/j.prime.2023.100108.

[4] K. Jha, A.G. Shaik, A comprehensive review of power quality mitigation in the scenario of solar PV integration into utility grid, e-Prime - Adv. Electr. Eng. Electron. Energy (2023), 100103, https://doi.org/10.1016/j.prime.2022.100103.

[5] D. Astiaso Garcia, G. Dionysis, P. Raskovic, N. Duić, M.A. Al-Nimr, Climate change mitigation by means of sustainable development of energy, water and environment systems, Energy Convers. Manag. X 17 (2022), https://doi.org/10.1016/j.ecmx.2022.100335. November.

[6] K.A. Abdulsalam, J. Adebisi, M. Emezirinwune, O. Babatunde, An overview and multicriteria analysis of communication technologies for smart grid applications, e-Prime - Adv. Electr. Eng. Electron. Energy 3 (2023), 100121, https://doi.org/10.1016/j.prime.2023.100121. January.

[7] L. Cioccolanti, R. Tascioni, R. Moradi, M. Pirro, C.M. Bartolini, I. Makhkamova, Kh. Mahkamov, L.F. Cabeza, A. De Gracia, P. Pili, A.C. Mintsa, D. Mullen, Development of a smart control unit for small-scale concentrated solar combined heat and power systems for residential applications, Electron. Energy 2 (2022), 100040, https://doi.org/10.1016/j.prime.2022.100040. March.

[8] D. Akinyele, I. Okakwu, E. Olabode, R. Blanchard, T. Ajewole, Integrated TEEP approach to microgrid design and planning with small hydro /solar / diesel resources for standalone application, e-Prime - Adv. Electr. Eng. Electron. Energy 2 (2022), 100091, https://doi.org/10.1016/j.prime.2022.100091. October.

[9] L. Herc, A. Pfeifer, F. Feijoo, N. Duić, Energy system transitions pathways with the new H2RES model: a comparison with existing planning tool, e-Prime - Adv. Electr. Eng. Electron. Energy (2021), 100024, https://doi.org/10.1016/j.prime.2021.100024.

[10] W. Chen, J.B. Ocreto, J.-.S. Wang, A.T. Hoang, J. Liou, Ch. Hwang, W.T. Chong, Two-stage optimization of three and four straight-bladed vertical axis wind turbines (SB-VAWT) based on Taguchi approach, Electron. Energy 1 (2021), 100025, https://doi.org/10.1016/j.prime.2021.100025. September.

[11] Z. Tang, A. Sangwongwanich, Y. Yang, F. Blaabjerg, Energy efficiency enhancement in full-bridge PV inverters with advanced modulations, e-Prime 1 (2021), 100004, https://doi.org/10.1016/j.prime.2021.100004. October.

[12] M.M. Rahman, E. Gemechu, A.O. Oni, A. Kumar, Energy and environmental footprints of flywheels for utility-scale energy storage applications, e-Prime 1 (2021), 100020, https://doi.org/10.1016/j.prime.2021.100020. October.

[13] K. Mahmoodi, H. Ghassemi, A. Razminia, Wind energy potential assessment in the Persian Gulf: a spatial and temporal analysis, Ocean Eng. 216 (2020), 107674, https://doi.org/10.1016/j.oceaneng.2020.107674. August 2019.

[14] G. Giebel and C.B. Hasager, An overview of offshore wind farm design, 2016, doi: 10.1007/978-3-319-39095-6.

[15] M.D. Esteban, J.J. Diez, J.S. López, V. Negro, Why offshore wind energy? Renew. Energy 36 (2011) https://doi.org/10.1016/j.renene.2010.07.009, 444–52011.

[16] Z.R. Shu, Q.S. Li, P.W. Chan, Investigation of offshore wind energy potential in Hong Kong based on Weibull distribution function, Appl. Energy 156 (2015) 362–373, https://doi.org/10.1016/j.apenergy.2015.07.027.

[17] Y.P. Liao, J.M. Kaihatu, The effect of wind variability and domain size in the Persian Gulf on predicting nearshore wave energy near Doha, Qatar, Appl. Ocean Res. 55 (2016) 18–36, https://doi.org/10.1016/j.apor.2015.11.012.

[18] J. Wang, X. Huang, Q. Li, X. Ma, Comparison of seven methods for determining the optimal statistical distribution parameters: a case study of wind energy assessment in the large-scale wind farms of China, Energy 164 (2018) 432–448, https://doi.org/10.1016/j.energy.2018.08.201.

[19] N. Aries, S.M. Boudia, H. Ounis, Deep assessment of wind speed distribution models: a case study of four sites in Algeria, Energy Convers. Manag. 155 (2018) 78–90, https://doi.org/10.1016/j.enconman.2017.10.082. August 2017.

[20] D. Mazzeo, G. Oliveti, E. Labonia, Estimation of wind speed probability density function using a mixture of two truncated normal distributions, Renew. Energy 115 (2018) 1260–1280, https://doi.org/10.1016/j.renene.2017.09.043.

[21] V. Katinas, G. Gecevicius, M. Marciukaitis, An investigation of wind power density distribution at location with low and high wind speeds using statistical model, Appl. Energy 218 (2018) 442–451, https://doi.org/10.1016/j.apenergy.2018.02.163. December 2017.

[22] J. Li, X. (Bill) Yu, Onshore and offshore wind energy potential assessment near Lake Erie shoreline: a spatial and temporal analysis, Energy 147 (2018) 1092–1107, https://doi.org/10.1016/j.energy.2018.01.118.

[23] A. Ucar, F. Balo, Investigation of wind characteristics and assessment of wind-generation potentiality in Uludağ-Bursa, Turkey, Appl. Energy 86 (3) (2009) 333–339, https://doi.org/10.1016/j.apenergy.2008.05.001.

[24] P.A. Costa Rocha, R.C. de Sousa, C.F. de Andrade, M.E.V. da Silva, Comparison of seven numerical methods for determining Weibull parameters for wind energy generation in the northeast region of Brazil, Appl. Energy 89 (1) (2012) 395–400, https://doi.org/10.1016/j.apenergy.2011.08.003.

[25] C.F. De Andrade, H.F. Maia Neto, P.A. Costa Rocha, M.E. Vieira Da Silva, An efficiency comparison of numerical methods for determining Weibull parameters for wind energy applications: a new approach applied to the northeast region of Brazil, Energy Convers. Manag. 86 (2014) 801–808, https://doi.org/10.1016/j.enconman.2014.06.046.

[26] S.M. Boudia, O. Guerri, Investigation of wind power potential at Oran, northwest of Algeria, Energy Convers. Manag. 105 (2015) 81–92, https://doi.org/10.1016/j.enconman.2015.07.055.

[27] B.H. Lee, D.J. Ahn, H.G. Kim, Y.C. Ha, An estimation of the extreme wind speed using the Korea wind map, Renew. Energy 42 (2012) 4–10, https://doi.org/10.1016/j.renene.2011.09.033.

[28] J.A. Carta, P. Ramírez, Use of finite mixture distribution models in the analysis of wind energy in the Canarian Archipelago, Energy Convers. Manag. 48 (1) (2007) 281–291, https://doi.org/10.1016/j.enconman.2006.04.004.

[29] J.A. Carta, P. Ramírez, S. Velázquez, A review of wind speed probability distributions used in wind energy analysis. Case studies in the Canary Islands, Renew. Sustain. Energy Rev. 13 (5) (2009) 933–955, https://doi.org/10.1016/j.rser.2008.05.005.

[30] C. Jung, D. Schindler, Global comparison of the goodness-of-fit of wind speed distributions, Energy Convers. Manag. 133 (2017) 216–234, https://doi.org/10.1016/j.enconman.2016.12.006.

[31] O.A. Jaramillo, M.A. Borja, Wind speed analysis in La Ventosa, Mexico: a bimodal probability distribution case, Renew. Energy 29 (10) (2004) 1613–1630, https://doi.org/10.1016/j.renene.2004.02.001.

[32] Q. Hu, Y. Wang, Z. Xie, P. Zhu, D. Yu, On estimating uncertainty of wind energy with mixture of distributions, Energy 112 (2016) 935–962, https://doi.org/10.1016/j.energy.2016.06.112.

[33] S.A. Akdağ, Ö. Güler, A novel energy pattern factor method for wind speed distribution parameter estimation, Energy Convers. Manag. 106 (2015) 1124–1133, https://doi.org/10.1016/j.enconman.2015.10.042.

[34] B. Kamranzad, A. Etemad-Shahidi, V. Chegini, Assessment of wave energy variation in the Persian Gulf, Ocean Eng. 70 (2013) 72–80, https://doi.org/10.1016/j.oceaneng.2013.05.027.

[35] M. Majidi Nezhad, M. Neshat, G. Piras, D. Astiaso Garcia, Sites exploring prioritisation of offshore wind energy potential and mapping for wind farms installation: iranian islands case studies, Renew. Sustain. Energy Rev. 168 (2022), 112791, https://doi.org/10.1016/j.rser.2022.112791. January.

[36] C.W. Zheng, C.Y. Li, J. Pan, M.Y. Liu, L.L. Xia, An overview of global ocean wind energy resource evaluations, Renew. Sustain. Energy Rev. 53 (667) (2016) 1240–1251, https://doi.org/10.1016/j.rser.2015.09.063.

[37] E. Berge, A.R. Gravdahl, J. Schelling, L. Tallhaug, O. Undheim, Wind in complex terrain. A comparison of WAsP and two CFD-models, Eur. Wind Energy Conf. Exhib. 2 (2006) 1569–1577, 2006, EWEC 2006.

[38] J. Waewsak, C. Kongruang, Y. Gagnon, Assessment of wind power plants with limited wind resources in developing countries: application to Ko Yai in southern Thailand, Sustain. Energy Technol. Assessments 19 (2017) 79–93, https://doi.org/10.1016/j.seta.2016.12.001.

[39] W. Promsen, I. Masiri, S. Janjai, Development of microscale wind maps for Phaluay Island, Thailand. Procedia Eng. 32 (2012) 369–375, 20122012.

[40] A. Chantelot, T. Clarenc, L. Corrochano, M. Alegre, W.T. Meteodyn, Site assessment in complex terrain, in: Proceedings of the EuropeanWind Energy Conference, Brussels, Belgium, 2008, 31 March –3 April 2008April2008.

[41] A.R. Gravdahl, K. Harstveit, WindSim – Flow simulations in complex terrain, Assess. Wind Resourc. Norwegian Coast (2019). Available online: https://windsim.com/documentation/papers_presentations/0006_dewek/dewek_2000_proceedings.pdf. accessed o, no. January2019.

[42] F. González-Longatt, J. Serrano González, M. Burgos Payán, J.M. Riquelme Santos, Wind-resource atlas of Venezuela based on on-site anemometry observation, Renew. Sustain. Energy Rev. 39 (2014) 898–911, https://doi.org/10.1016/j.rser.2014.07.172.

[43] S. Proietti, P. Sdringola, F. Castellani, D. Astolfi, E. Vuillermoz, On the contribution of renewable energies for feeding a high altitude Smart Mini Grid, Appl. Energy 185 (2017) 1694–1701, https://doi.org/10.1016/j.apenergy.2015.12.056.

[44] R. Dutra, A. Szklo, Assessing long-term incentive programs for implementing wind power in Brazil using GIS rule-based methods, Renew. Energy 33 (12) (2008) 2507–2515, https://doi.org/10.1016/j.renene.2008.02.017.

[45] A. Agüera-Pérez, J.C. Palomares-Salas, J.J. González de la Rosa, J.G. Ramiro-Leo, A. Moreno-Muñoz, Basic meteorological stations as wind data source: a mesoscalar test, J. Wind Eng. Ind. Aerodyn. 107–108 (2012) 48–56, https://doi.org/10.1016/j.jweia.2012.03.020.

[46] T. Ishihara, a. Yamaguchi, Y. Fujino, Development of a new wake model based on a wind tunnel experiment, Glob. Wind Power (2004) 6. March 2016[Online]. Available: http://windeng.t.u-tokyo.ac.jp/ishihara/posters/2004_gwp_poster.pdf%5Cnhttp://windeng.t.u-tokyo.ac.jp/ishihara/proceedings/2004-5_poster.pdf.

[47] R.J. Barthelmie, K. Hansen, S.T. Frandsen, O. Rathmann, J.G. Schepers, W. Schlez, J. Phillips, K. Rados, A. Zervos, E.S. Politis, P.K. Chaviaropoulos, Modelling and measuring flow and wind turbine wakes in large wind farms offshore, Wind Energy 12 (5) (2009) 431–444, https://doi.org/10.1002/we.348.

[48] N.O. Jensen, A note on wind generator interaction, Risø-M-2411 Risø Natl. Lab, Roskilde (1983) 1–16 [Online]. Available: http://www.risoe.dk/rispubl/VEA/veapdf/ris-m-2411.pdf.

[49] S. Ivanell, R.F. Mikkelsen, J.N. Sørensen, K.S. Hansen, D. Henningson, The impact of wind direction in atmospheric BL on interacting wakes at Horns Rev wind farm, Torque (2010) 407–426, 2010[Online]. Available: http://bit.ly/14SDTwj.

[50] S. Ott, J. Berg, and M. Nielsen, Linearised CFD Models for Wakes, 2011.
[51] F. Porte-Agel, Y.T. Wu, C.H. Chen, A numerical study of the effects of wind direction on turbine wakes and power losses in a large wind farm, Energies 6 (10) (2013) 5297–5313, https://doi.org/10.3390/en6105297.
[52] A. Kalmikov, G. Dupont, K. Dykes, C. Chan, Wind power resource assessment in complex urban environments: MIT campus case-study using CFD Analysis, in: Awea 2010 Wind. Conf., 2010, p. 2010. March.
[53] A.Z. Dhunny, M.R. Lollchund, S.D.D.V. Rughooputh, Numerical analysis of wind flow patterns over complex hilly terrains: comparison between two commonly used CFD software, Int. J. Glob. Energy Issues 39 (3–4) (2016) 181–203, https://doi.org/10.1504/IJGEI.2016.076339.
[54] D. Carvalho, A. Rocha, C.S. Santos, R. Pereira, Wind resource modelling in complex terrain using different mesoscale-microscale coupling techniques, Appl. Energy 108 (2013) 493–504, https://doi.org/10.1016/j.apenergy.2013.03.074.
[55] J.M.L.M. Palma, F.A. Castro, L.F. Ribeiro, A.H. Rodrigues, A.P. Pinto, Linear and nonlinear models in wind resource assessment and wind turbine micro-siting in complex terrain, J. Wind Eng. Ind. Aerodyn. 96 (12) (2008) 2308–2326, https://doi.org/10.1016/j.jweia.2008.03.012.
[56] F. Castellani, D. Astolfi, M. Burlando, L. Terzi, Numerical modelling for wind farm operational assessment in complex terrain, J. Wind Eng. Ind. Aerodyn. 147 (2015) 320–329, https://doi.org/10.1016/j.jweia.2015.07.016.
[57] D. Tabas, J. Fang, F. Porté-Agel, Wind energy prediction in highly complex terrain by computational fluid dynamics, Energies 12 (7) (2019) 1–12, https://doi.org/10.3390/en12071311.
[58] H.R. Bargahi, M.R. Shokri, F. Kaymaram, M.R. Fatemi, Changes in reef fish assemblages following multiple bleaching events in the world's warmest sea (Kish Island, the Persian Gulf), Coral. Reefs 39 (3) (2020) 603–624, https://doi.org/10.1007/s00338-020-01945-3.
[59] S.J. Brandl, J.L. Johansen, J.M. Casey, L. Tornabene, R.A. Morais, J.A. Burt, Extreme environmental conditions reduce coral reef fish biodiversity and productivity, Nat. Commun. 11 (1) (2020) 1–14, https://doi.org/10.1038/s41467-020-17731-2.
[60] Y. Alosairi, N. Alsulaiman, A. Rashed, D. Al-Houti, World record extreme sea surface temperatures in the northwestern Arabian/Persian Gulf verified by in situ measurements, Mar. Pollut. Bull. 161 (2020), 111766, https://doi.org/10.1016/j.marpolbul.2020.111766. October.
[61] K.O. Emery, (2), Sediments and Water of Persian Gulf, Am. Assoc. Pet. Geol. Bull. 40 (10) (1956) 2354–2383, https://doi.org/10.1306/5ceae595-16bb-11d7-8645000102c1865d.
[62] M.I. El-Sabh, T.S. Murty, Storm surges in the Arabian Gulf, Nat. Hazards 1 (4) (1989) 371–385, https://doi.org/10.1007/BF00134834.
[63] A. Merlone, H. Al-Dashti, N. Faisal, R.S. Cerveny, S. Al Sarmi, P. Bessemoulin, M. Brunet, F. Driouech, Y. Khalatyan, T.C. Peterson, F. Rahimzadeh, B. Trewin, M. M. Abdel Wahab, S. Yagan, G. Coppa, D. Smorgon, Ch. Musacchio, D. Krahenbuhl, Temperature extreme records: world Meteorological Organization metrological and meteorological evaluation of the 54.0 °C observations in Mitribah, Kuwait and Turbat, Pakistan in 2016/2017, Int. J. Climatol. 39 (13) (2019) 5154–5169, https://doi.org/10.1002/joc.6132.
[64] M.A. Alkhalidi, S.K. Al-dabbous, S. Neelamani, H.A. Aldashti, Wind energy potential at coastal and offshore locations in the state of Kuwait, Renew. Energy 135 (2019) 529–539, https://doi.org/10.1016/j.renene.2018.12.039.
[65] S. Neelamani, K. Rakha, K. Al-Salem, M. Al-Khaldi, Extreme wave heights in the Kuwaiti territorial waters based on 12- and 15-year data, Kuwait J. Sci. Eng. 39 (1 A) (2012) 193–210.
[66] W. Al-Nassar, S. Alhajraf, A. Al-Enizi, L. Al-Awadhi, Potential wind power generation in the State of Kuwait, Renew. Energy 30 (14) (2005) 2149–2161, https://doi.org/10.1016/j.renene.2005.01.002.
[67] J.P. Arenas-López, M. Badaoui, Analysis of the offshore wind resource and its economic assessment in two zones of Mexico, Sustain. Energy Technol. Assessments 52 (2022), https://doi.org/10.1016/j.seta.2022.101997. September 2021.
[68] J. Benesty, J. Chen, Y. Huang, I. Cohen, Pearson Correlation Coefficient, 2, Springer Top. Signal Process, 2009, pp. 1–4, https://doi.org/10.1007/978-3-642-00296-0_5.
[69] A. Monti, A proposal for a residual autocorrelation test in linear models, Biometrika 81 (1994) 776–780.
[70] D.Y.C. Leung, Y. Yang, Wind energy development and its environmental impact: a review, Renew. Sustain. Energy Rev. 16 (1) (2012) 1031–1039, https://doi.org/10.1016/j.rser.2011.09.024.
[71] C. Lavanya, N.D. Kumar, Foundation types for land and offshore sustainable wind energy turbine towers, in: E3S Web Conf. 184, 2020, pp. 1–6, https://doi.org/10.1051/e3sconf/202018401094.
[72] Z. Jiang, Installation of offshore wind turbines: a technical review, Renew. Sustain. Energy Rev. 139 (2021), 110576, https://doi.org/10.1016/j.rser.2020.110576. August 2020.
[73] K.Y. Oh, W. Nam, M.S. Ryu, J.Y. Kim, B.I. Epureanu, A review of foundations of offshore wind energy convertors: current status and future perspectives, Renew. Sustain. Energy Rev. 88 (2018) 16–36, https://doi.org/10.1016/j.rser.2018.02.005. February 2017.
[74] X. Li, X. Zeng, X. Yu, X. Wang, Seismic response of a novel hybrid foundation for offshore wind turbine by geotechnical centrifuge modeling, Renew. Energy 172 (2020) 1404–1416, https://doi.org/10.1016/j.renene.2020.11.140.
[75] B.W. Byrne, G.T. Houlsby, Foundations for offshore wind turbines, Philos. Trans. R. Soc. A Math. Phys. Eng. Sci. 361 (1813) (2003) 2909–2930, https://doi.org/10.1098/rsta.2003.1286.
[76] G.T. Houlsby, B.W. Byrne, and C.M. Martin, Novel Foundations for Offshore Wind Farms, no. August 2001.
[77] https://orsted.com/en/what-we-do/renewable-energy-solutions/offshore-wind/wind-technology/suction-bucket-jacket-foundations. 2023.
[78] BOEM, Comparison of environmental effects from different offshore wind turbine foundations, pp. 1–42, 2020, [Online]. Available: https://www.boem.gov/sites/default/files/documents/environment/Wind-Turbine-Foundations-White Paper-Final-White-Paper.pdf.
[79] M. Hannon, E. Topham, J. Dixon, D. Mcmillan, M. Collu, Offshore wind, ready to float?. Global and UK Trends in the Floating Offshore Wind Market, 2019, https://doi.org/10.17868/69501. October.
[80] B. Fenu, V. Attanasio, P. Casalone, R. Novo, G. Cervelli, M. Bonfanti, S.A. Sirigu, G. Bracco, G. Mattiazzo, Analysis of a gyroscopic-stabilized floating offshore hybrid wind-wave platform, J. Mar. Sci. Eng. 8 (6) (2020) 439, https://doi.org/10.3390/jmse8060439.
[81] Fincantieri Offshore: Sea flower platform, no. September, p. Available online: https://www.fincantieri offshore., 2020.
[82] https://www.principlepower.com/projects/windfloat-atlantic. 2023.
[83] A. Roddier, D. Cermelli, C. Weinstein, Windfloat: a floating foundation for offshore wind turbines. Part 1: design basis and qualification process, in: Proc. ASME 28th Int. Conf. Ocean. Offshore Arct. Eng, Honolulu, HI, US, 2009. June2009.
[84] https://www.windfloat-atlantic.com/the-wind-farm/. 2023.
[85] https://www.equinor.com/energy/hywind-tampen. 2023.
[86] Equinor, HyWind Scotland, The World's first commercial floating wind farm, no. October, p. Available online: https://www.equinor.com/en/what, 2020.
[87] https://www.saipem.com/sites/default/files/2022-09/Floating%20offshore%20wind.pdf. 2023.

Dr. Eng. Meysam Majidi Nezhad: Meysam obtained his Ph.D. in the Energy and Environment Department of Astronautics, Electrical and Energetics Engineering (DIAEE), Sapienza University of Rome, Italy. His research fields are energy planning, renewable energy source analysis, and satellite remote sensing. He is a remote sensing of energy and environment expert with research experience at the Department for Sustainable Energy Systems, Mälardalens University, Sweden, and DIAEE / CITERA Interdepartmental Research Center Territory Building Restoration Environment, the Sapienza University of Rome. He has collaborated on several EU Horizon 2020 projects.

Dr. Mehdi Neshat: He received the Ph.D. degree in Computer Science, from the University of Adelaide, Australia, in 2020. From 2020 to 2023, he has been a Postdoctoral Research Associate in Data Science, Machine learning, and Deep learning with the University of South Australia. He is also an Adjunct Research Fellow at the Center for Artificial Intelligence Research and Optimization, Torrens University Australia, Australia. His primary research interests include Artificial Intelligence, Optimization, and Machine /Deep learning.

Dr. Maher Azaza: Maher Azaza, senior lecturer in energy engineering at Mälardalens University, obtained his PhD degree in Electronics at the faculty of Sciences of Tunis. His research focuses on the optimal energy usage at the demand side, basically in the buildings sector, and how renewables technologies can be optimally integrated to further promote energy system decarbonization.

Dr. Anders Avelin: Anders obtained his PhD degree in Energy and Environmental Engineering at Mälardalens University, His research fields are in process diagnostics connected to Heat and power generation and the pulp and paper industry. feed-forward model-predictive control for the pulp and paper industry including the development of NIR-based soft sensors for such applications. Focusing on the use of physics-based algorithms and simulation techniques and hybrid solutions coupled with machine learning techniques. Anders has a long industry experience in the energy sector.

Prof. Giuseppe Piras: He conducts research in the fields of building production, civil energy, and environmental control, his work focuses on building energy efficiency and automated-digital management of microgeneration networks.

Since 2001 he is a professor of Technical Environmental Physics at Sapienza University of Rome.

Since 2010 he is a professor at the School of Specialization in Architectural and Landscape Heritage at Sapienza University of Rome.

Director of the Master in “Integrated management and valorization of real estate and urban assets - Asset, property, facility & energy management” at Sapienza University of Rome.

Member of the Scientific Council of the Master in “Building Information Modeling” and in “Innovation Engineering”.

Lab head TEECLAB, Technologies for energetic and environmental control.

Member of the Board of the PhD program "Energy and Environment".

Member of the Executive Board of CITERA research center.

Management Representative of Team Sapienza Solar Decathlon Middle East 2018

Former member of the Academic Senate of Sapienza University of Rome.

Former Coordinator for Energy saving and Environmental control of the Sapienza University of Rome.

Former Member of the Scientific Research Commission of Sapienza University of Rome.

Former Member of the research group at the Research center for the Causes of Decay of Artistic and Monumental Heritage, Sapienza-CNR.

Prof. Davide Astiaso Garcia: Davide Astiaso Garcia is Associate Professor of Thermal Sciences, Energy Technology and Building Physics at Sapienza University of Rome and is the Secretary General of the Italian Wind Energy Association (ANEV).

His full operating skills include, among others: Wind Energy, other renewable energies, smart energy systems, energy efficiency in buildings.

He has a body of funded research comprising over €2.5 M in European research projects on competitive funds.

In particular, he has participated in more than 15 European (Horizon 20202, Interreg Med, ENPI CBC Med, Erasmus+) and national research projects in the field of renewable energies and smart energy systems (in many cases as Principal Investigator and Project Coordinator). He is awarded with the national scientific qualification as Full Professor.

Since 2019, he is included in the World’s Top 2% Scientists List in the Energy field both for the whole carrier and for the last year publications according to the "Updated science-wide author databases of standardized citation indicators" Elsevier and SciTech Strategies (Stanford University).